# Extending the Sensing Range of Brillouin Optical Time-Domain Analysis Combining Frequency-Division Multiplexing and In-Line EDFAs

Yongkang Dong, *Member, IEEE, OSA*, Liang Chen, and Xiaoyi Bao, *Senior Member, IEEE*

*(Invited Paper)*

***Abstract*—We demonstrate a high-performance Brillouin optical time-domain analysis (BOTDA) system with an extended sensing range by combining frequency-division multiplexing and in-line Erbium doped fiber amplifiers (EDFAs). The frequency-division multiplexing BOTDA features multiple sections of fibers with different Brillouin frequency shifts, and it reduces the effective Brillouin interaction length to one resonant Brillouin frequency section rather than the entire length of the sensing fiber, so that the power of CW probe of BOTDA can be increased to enhance the Brillouin signal within individual sections and consequently extend the sensing range combined with high strain or temperature resolution with negligible pump depletion. In addition, in-line EDFAs placed between spans are used to compensate the fiber loss for similar Brillouin gains in each span. In experiment, a 150-km sensing range is achieved by dividing the sensing fibers into two spans of equal length and using two types of fibers in each span. Using the differential pulse-width pair technique, a 100/120 ns pulse pair is used to realize a 2-m spatial resolution and a measurement accuracy of 1.5°C/30 $\mu\varepsilon$ at the end of the sensing fibers.**

***Index Terms*—Brillouin sensor, erbium doped fiber amplifier, frequency-division multiplexing, strain and temperature measurement.**

## I. Introduction

THE high-performance and long-range Brillouin distributed optical fiber sensors have gained considerable interests because of their capabilities of monitoring strain and temperature of large-scale structures. Usually, a pump pulse and a continuous-wave (CW) probe are included in a Brillouin-gain based Brillouin optical time-domain analysis (BOTDA) scheme, and the Brillouin gain spectra over the sensing fiber are obtained through scanning their frequency offset in the vicinity of the Brillouin frequency shift (BFS). When it comes to a long sensing range, due to the fiber attenuation both pump pulse and CW probe powers need to be increased to get an adequate signal-to-noise ratio (SNR) over the entire sensing fiber, which, however, can induce some nonlinear effects, such as pump depletion [1] and modulation instability (MI) [2], and consequently limits the extending of the sensing range. The pump depletion refers to that when the frequency offset between the pump and probe waves equals to the BFS of the sensing fiber a considerable portion of the pump power is transferred to the CW probe wave, which not only decreases the Brillouin gain but also makes the pulsed pump power unequally depleted for different frequency offsets at the far end of the sensing fiber, resulting in distorted Brillouin spectra and systematic measurement errors. The pump depletion will be maximized for the worst case when the sensing fiber has a uniform BFS. Similarly, excess amplification in a Brillouin-loss based sensor can also lead to distorted Brillouin spectra and systematic measurement errors at the far end of the sensing fiber [3], [4]. In addition, MI effect is another limitation factor for extending the sensing range, by which the spectrum of the pump pulse can be considerably broadened with a high peak power and thus sharply decreases the Brillouin signal in a long standard single mode fiber (SMF) with abnormal dispersion (positive dispersion parameter), while fortunately it can be effectively removed by using a negative dispersion fiber [2], [4].

To address these issues and extend the sensing range, several techniques have been recently proposed to realize a long-range and high-performance BOTDA system. Optical pulse coding technique, which decreases the power requirement over pump pulse and hence can reduce pump depletion and avoid MI effect, was introduced into BOTDA to improve the SNR realizing 1-m [5] and 0.5-m [6] spatial resolution over 50-km length, respectively. Combined optical pulse coding and a pre-amplifier before the detector, the sensing range was extended to 120 km with a 3-m spatial resolution [7]. Another technique is to use Raman amplifiers to extend the sensing range [8]–[10], where pump depletion and MI effect could be avoided because low pump and probe powers are needed with the fiber attenuation compensated by the distributed Raman gain. With optimized parameters a 120-km sensing range with a 2-m spatial resolution was realized by using a bidirectional in-line Raman amplifier [10]. Another technique to extend the sensing range is to reduce the pump depletion via restricting the pump and probe overlapping time realized by time-division multiplexing for one measurement, based on which a 100-km sensing range with a 2-m

Manuscript received June 21, 2011; revised August 23, 2011; accepted September 22, 2011. Date of publication October 06, 2011; date of current version March 14, 2012. This work was supported in part by the Natural Science and Engineering Research Council of Canada through discovery and strategic grant and in part by Canada Research Chair Program.

The authors are with the Department of Physics, University of Ottawa, Ottawa, ON K1N 6N5, Canada (e-mail: aldendong@gmail.com; Liang.Chen@uottawa.ca; xbao@uottawa.ca).

Digital Object Identifier 10.1109/JLT.2011.2170813

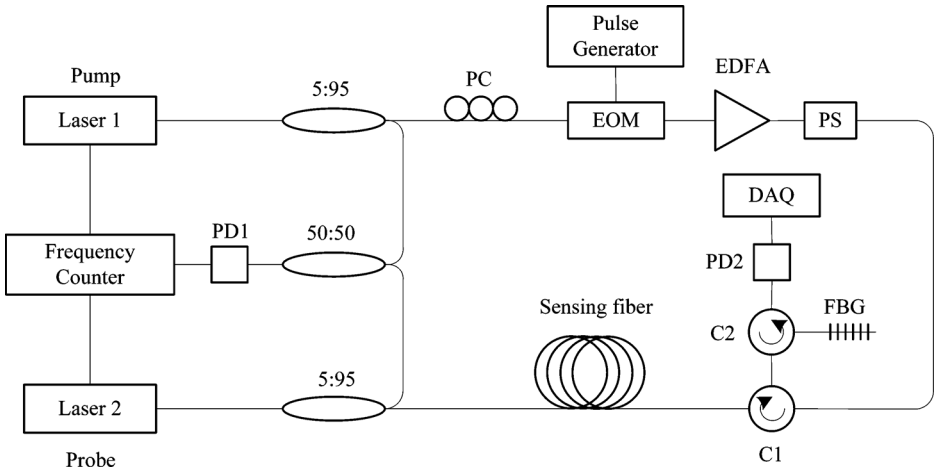


Fig. 1. Experimental setup. PD: photo-detector, PC: polarization controller, PS: polarization scrambler, EOM: electro-optic modulator, EDFA: Erbium-doped fiber amplifier, C: circulator, DAQ: data acquisition, FBG: fiber Bragg grating.

spatial resolution was realized without in-line amplifiers [11]. In addition, a so-called double-sideband configuration, which includes both Stokes and anti-Stokes components in the CW probe wave, can partly reduce the pump depletion effect, and was applied in Brillouin optical frequency-domain analysis (BOFDA) [12] and BOTDA [5], [7], [10], [13]. However, due to the unbalanced energy transfer of the two processes in different fiber locations, i. e., Stokes/Pump and Pump/anti-Stokes, which could be caused by high-gains by a high pump power and different changes state of polarization for Stokes and antiStokes waves, the pump depletion can not be completely removed.

In this paper, we demonstrate an extended sensing range of BOTDA through combining frequency-division multiplexing and in-line Erbium doped fiber amplifiers (EDFAs) to reduce the pump depletion and compensate the fiber attenuation, respectively. The frequency-division multiplexing BOTDA features multiple sections with different BFSs in sensing fibers, so that the effective Brillouin interaction length is restricted to one resonant Brillouin frequency section rather than the entire sensing length, thus pump depletion can be considerably reduced [14]. In-line EDFAs are used in the middle of the sensing fibers to compensate the fiber loss on both pump and probe waves, so that similar Brillouin gains and SNR can be obtained in both two spans. In addition, because the sensing fiber includes different types of fibers with different BFSs, the spontaneous Brillouin scattering can not accumulate over the whole sensing fiber, which is another advantage of frequency-division multiplexing. This is particularly important for EDFA based BOTDA sensor, as well as Raman based BOTDA, in which amplified spontaneous Brillouin scattering noise can be reduced significantly.

## II. Experimental Setup

The experimental setup is shown in Fig. 1. Two narrow linewidth (3 kHz) fiber lasers operating at 1550 nm are used to provide the pump and probe waves, respectively, whose frequency difference is locked by a microwave frequency counter and is automatically swept by varying the temperature of the fiber Bragg grating (FBG) of the cavity controlled by a computer. A 12-GHz bandwidth high-speed detector is used to measure the beating signal of the pump and probe waves, which provides feedback to the frequency counter to lock their frequency difference. The pump laser is launched into a high extinction-ratio (ER) electro-optic modulator (EOM) to create a pump pulse with the ER higher than 45 dB. Before launched into the sensing fiber, the pump pulse is amplified by an EDFA. A polarization scrambler is used to continuously change the polarization state of the pump pulse to reduce the polarization-dependent fluctuation on the signal by averaging a large number of signals, where an averaging number of 2000 is used in our experiment. A FBG with a 3-dB bandwidth of 0.03 nm is used in front of the detector to filter out the Rayleigh scattering noise of the pump pulse.

## III. 75-km Sensing Range Based on Frequency-Division Multiplexing

### A. Layout of the Sensing and Leading Fibers

We first perform a 75-km sensing range based on frequency-division multiplexing by using three types of fibers, which are MetroCor, LEAF and SMF-28, respectively. The measured fiber attributes are listed in Table I. Because of the relative small mode field area (MFA) of $\sim$50 $\mu$m$^2$, MetroCor fiber has the maximum Brillouin gain. The effective MFA for LEAF and SMF-28 are 72.2 and 83.7 $\mu$m$^2$, respectively. However, LEAF fiber has the smallest Brillouin gain because of the much smaller overlapping of the electric and acoustic fields in it [15]. The BFS differences at room temperature (25°C) between MetroCor and LEAF, and LEAF and SMF-28 are 127 and 222 MHz, respectively, which are both much larger than Brillouin gain bandwidth ($\sim$30 MHz in silica fibers). Large BFS differences among these fibers ensure that the Brillouin interaction can occur within only one resonant section at one time; hence the CW probe power can be increased to improve the SNR without pump depletion. The measurement for the entire sensing fiber is realized by combining the series measurements over different sections, and different scanning frequency ranges should be applied for individual sections, which accounts for the definition of frequency-division multiplexing in this paper.

TABLE I
MEASURED FIBER ATTRIBUTES

| Fiber type | $g_B/A_{eff}$ ($W^{-1}m^{-1}$)[a] | BFS (MHz) | Dispersion (ps/(nm·km)) |
|---|---|---|---|
| MetroCor | 0.1669 | 10518 | -10~ -1 |
| LEAF | 0.0892 | 10645 | 2~6 |
| SMF-28 | 0.1281 | 10867 | 16~19 |

a These are average gains with scrambling the polarization state of the probe wave.

TABLE II
FITTING ERRORS ($\delta\upsilon_B$) AND BRILLOUIN LINE-WIDTHS ($\Delta\upsilon_B$) FOR FIG. 9

| Position (km) | Parameter | Span 1 (MHz) | Span 2 (MHz) |
|---|---|---|---|
| 25 | $\delta\upsilon_B$ | 0.13 | 0.33 |
| | $\Delta\upsilon_B$ | 38 | 43.8 |
| 50 | $\delta\upsilon_B$ | 0.42 | 0.63 |
| | $\Delta\upsilon_B$ | 37.8 | 42.9 |
| 75 | $\delta\upsilon_B$ | 1.24 | 1.49 |
| | $\Delta\upsilon_B$ | 28.4 | 34.2 |

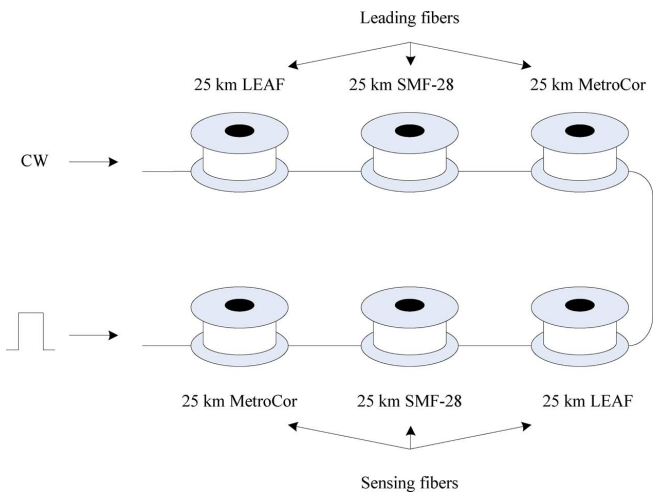


Fig. 2. Layout of the sensing and leading fibers for a 75-km sensing range based on frequency-division multiplexing.

The layout of the sensing and leading fibers, both composed of a 25-km MetroCor fiber, a 25-km SMF-28 fiber and a 25-km LEAF fiber, is shown in Fig. 2. Usually, for a BOTDA scheme, two ends of the sensing fiber should be accessed and the pump pulse goes a round-trip, which makes the effective sensing range be only half of the fiber length. To realize an actual 75-km sensing range, a 75-km leading fiber is used to deliver the CW probe to the far end of the sensing fiber. Using three types of fibers with different BFSs increases the SBS threshold and thus ensures delivering sufficient CW probe power to the sensing fiber. The 25-km LEAF fiber with the minimum Brillouin gain is placed in the front end of the leading fiber ensuring the maximum SBS threshold. The total loss (including splice loss) of the 75-km leading fiber is measured to be 16 dB. A CW probe with a power of 10 mW, which is lower than the SBS threshold, is launched into the leading fiber with 0.25 mW left when entering the sensing fibers.

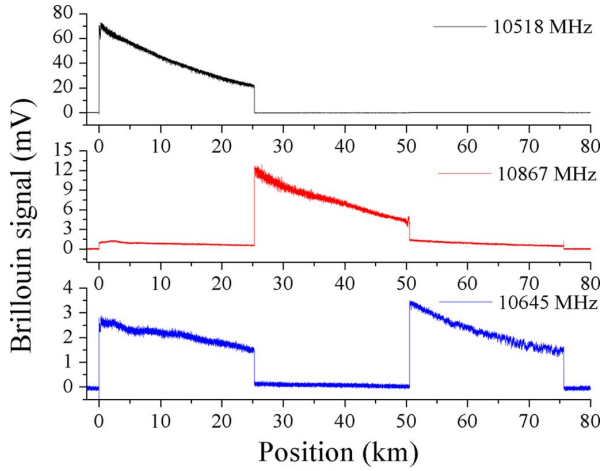


Fig. 3. Time traces of Brillouin signal at different frequency offsets of 10518, 10867 and 10645 MHz with a 40-ns pump pulse.

In terms of the propagation direction of the pump pulse, the sensing fiber is composed of MetroCor, SMF-28 and LEAF fibers in sequence. A high-power pump pulse is preferable to improve the SNR. However, the maximum input pump pulse power is limited by the MI effect in a positive dispersion fiber, such as LEAF and SMF-28. To address this issue, a 25-km MetroCor fiber with negative dispersion is placed in the front end of the sensing fiber to avoid MI effect within this section. Because of the fiber attenuation, the pump pulse power could be lower than the MI threshold for the following two positive dispersion fibers. A pump pulse of 800 mW is used, which is lower than the MI threshold of the sensing fibers. The Brillouin gain parameters should be kept in a low level in each section to reduce pump depletion [4]. Neglecting the pump depletion, the Brillouin gain parameter is given by $G = g_B P L_{\text{eff}}/A_{\text{eff}}$, where $g_B$ is the Brillouin gain coefficient, $P$ is the CW wave power at the start-end of the individual sections, $L_{\text{eff}}$ is the effective length, and $A_{\text{eff}}$ is the effective core area. The calculated Brillouin gain parameters for the LEAF, SMF-28 and MetroCor fibers, which are all 25 km in length, are 0.34, 0.12 and 0.05, respectively. These small Brillouin gain parameters ensure non-distorted Brillouin spectra for the entire sensing fiber.

### *B. Measurement Results*

Because of the different BFSs for individual sections, different scanning frequency ranges are required correspondingly for the measurement of each section. The time traces of Brillouin signal at different frequency offsets of 10518, 10867 and 10645 MHz are shown in Fig. 3, where the pump pulsewidth is 40 ns. The black curve shows the signal of MetroCor fiber in the first 25-km section and the red curve shows the signal of SMF-28 fiber in the second 25-km section. For the blue curve, besides the signal of LEAF fiber in the third 25-km section, the signal of MetroCor fiber is also observed. However, in this case the pump pulse depletion in the first 25-km fiber can be negligible due to very small CW probe power in this section. No MI effect is observed in any of these fibers, and the Brillouin signal decreasing of each section is only contributed by the fiber attenuation.

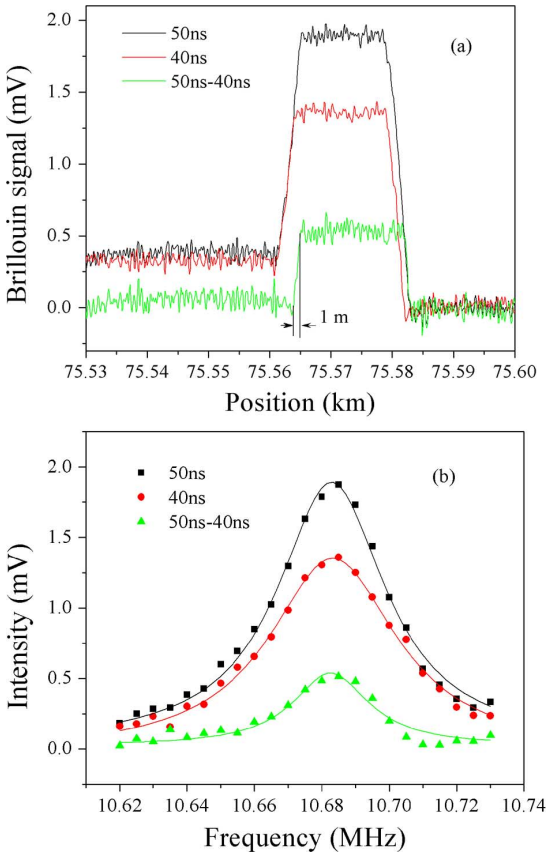


Fig. 4. (a) Time traces of Brillouin signal and (b) typical Brillouin spectra of the heated fiber near the end of 75 km sensing fiber.

A 40-ns pump pulse defines a 4-m spatial resolution, and the spatial resolution can be further improved by using a differential pulse-width pair (DPP) in BOTDA [16]–[18]. The DPP-BOTDA is implemented as follows: first, two time traces of Brillouin signal are obtained by using two pulses with different pulse-widths, respectively; second, the differential signal is obtained by taking subtraction between the two Brillouin signals, and then the differential Brillouin spectra can be obtained by sweeping the frequency offset in the vicinity of the BFS. In the differential Brillouin spectra, the spatial resolution is determined by the differential pulse, i.e., the pulse-width difference of the pulse pair, rather than the original pulses.

Near the end of the 75-km sensing fiber, an 18-m segment was heated to 65°C in an oven. Fig. 4(a) gives the time traces of Brillouin signal with 40 and 50 ns pump pulses and their differential signal, where the frequency offset was set at the BFS of the heated fiber, i.e., 10685 MHz. The rising edge of transition region of the differential signal defines a spatial resolution of 1 m. Typical Brillouin spectra of the heated fiber with 40 and 50 ns pump pulse and their differential spectrum are plotted in Fig. 4(b), where the Brillouin spectra match well with a Lorentz profile with only very slight distortion indicating that the pump depletion can be negligible. The standard deviation of the differential Brillouin spectrum is 1 MHz, which corresponds to an accuracy of 1°C or 20 $\mu\varepsilon$.

We then carried out a measurement near the end of 50 km of the sensing fiber, where two 2-m segments were stretched with a 1-m segment under loose condition in between. The measured

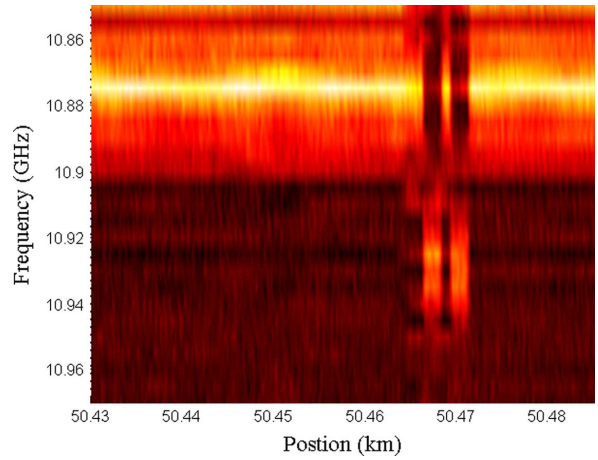


Fig. 5. Top-view of the three-dimensional Brillouin spectra near the end of 50 km with a 46/50 ns pulse pair. Two 2-m segments are stretched with a 1-m segment under loose condition in between.

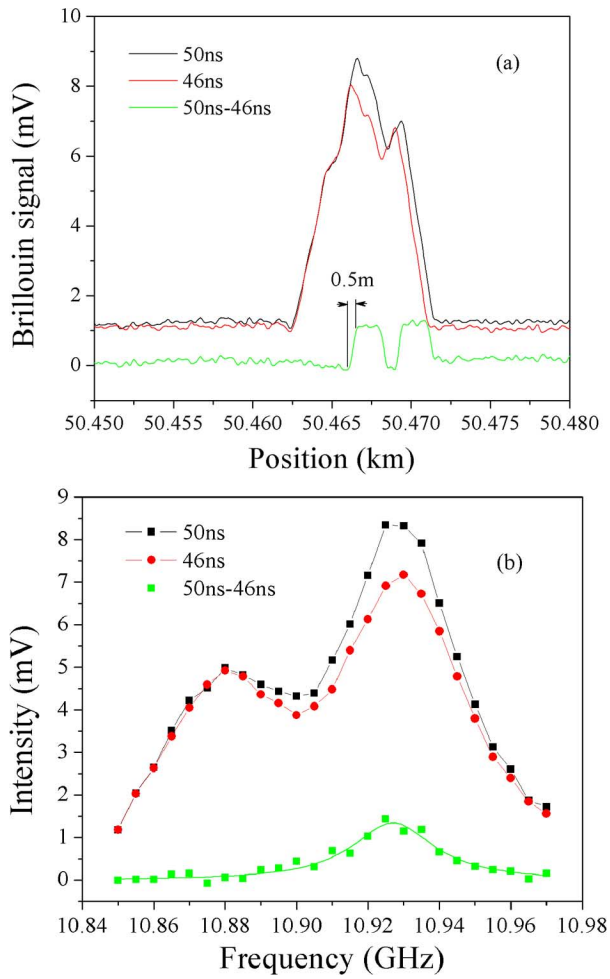


Fig. 6. (a) Time traces of Brillouin signal and (b) typical Brillouin spectra of the stretched fiber near the end of 50 km sensing fiber.

three-dimensional Brillouin spectra using a 46/50 ns pulse pair are shown in Fig. 5, where the two stretched segments can be clearly distinguished. They are also clearly seen in the time trace of the differential Brillouin signal shown as the green curve in Fig. 6(a), where the rising edge of transition region of the differential signal defines a spatial resolution of 0.5 m.

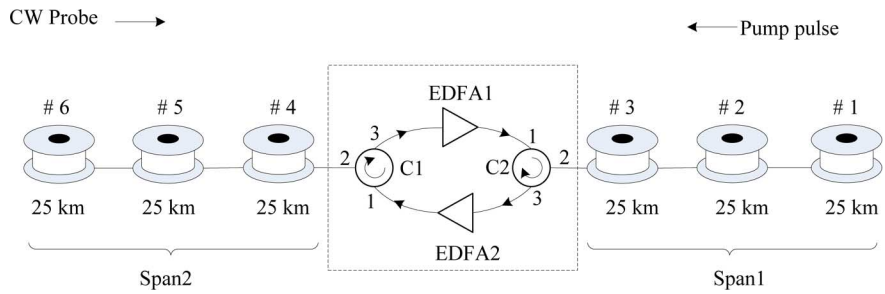


Fig. 7. Layout of the sensing fibers and in-line EDFAs. C: circulator.

The measured Brillouin spectra of the stretched fiber with 46 and 50 ns pump pulse and their differential spectrum are plotted in Fig. 6(b). Limited by the spatial resolution, the spectra with 46-ns and 50-ns pulses both feature two peaks, where the right peak corresponds to the stretched fiber, while the left one is caused by the cross-talking of the non-stretched fiber. However, the differential Brillouin spectrum exhibits only one peak corresponding to the stretched fiber. The standard deviation of the differential Brillouin spectrum is 0.7 MHz, which corresponds to an accuracy of 0.7°C or 14 $\mu\varepsilon$.

## IV. 150-km Sensing Range Combining Frequency-Division Multiplexing and In-Line EDFAs

### A. Layout of the Sensing Fibers and In-Line EDFAs

EDFAs have been successfully and widely deployed to compensate the fiber attenuation in the long-haul transmission system, so that many thousands of km long optical fiber networks have been possible. To further extend the sensing range of BOTDA, we use in-line EDFAs placed between two spans to amplify the pump and probe waves and compensate the fiber attenuation, while frequency-division multiplexing is applied in each span to reduce the pump depletion.

Fig. 7 shows the layout of the sensing fibers and in-line EDFAs for a 150-km sensing range, where the sensing fibers are divided into two spans of equal length of 75 km with the span 1 consisting of spools 1 to 3 and the span 2 consisting of spools 4 to 6. Between the two spans is an optical repeater consisting of two in-line EDFAs and two optical circulators as shown in the dashed frame in Fig. 7. The pump and probe waves can be amplified separately as they pass through their own branches of the optical repeater: in the probe branch, the probe wave goes from port 2 to port 3 of optical circulator 1, and after amplified by EDFA1 goes from port 1 to port 2 of circulator 2 entering the span 1; in the pump branch, the pump wave goes from port 2 to port 3 of circulator 2, and after amplified by EDFA2 goes from port 1 to port 2 of optical circulator 1 entering the span 2. In this scheme, since only two spans and one optical repeater are included, ASE noise from the in-line EDFAs does not have considerable impact on the performance. However, if many spans are used ASE noise for both branches should be in-line filtered to avoid ASE noise accumulating, which may saturate the in-line EDFAs and thus decrease the gain for signals.

Two types of fibers are included in each span to reduce the pump depletion based on frequency-division multiplexing, i.e., a 50-km MetroCor fiber (consisting of two 25-km spools) and a 25-km LEAF fiber, where the MetroCor fiber with negative dispersion is placed in the front end of the sensing fiber to avoid the MI effect. As it is shown in Fig. 7, the spools 3 and 6 are LEAF fiber and the rest are MetroCor fiber. The BFSs at room temperature for spool 1 to 6 are measured to be 10518, 10573, 10643, 10540, 10525 and 10646 MHz, respectively.

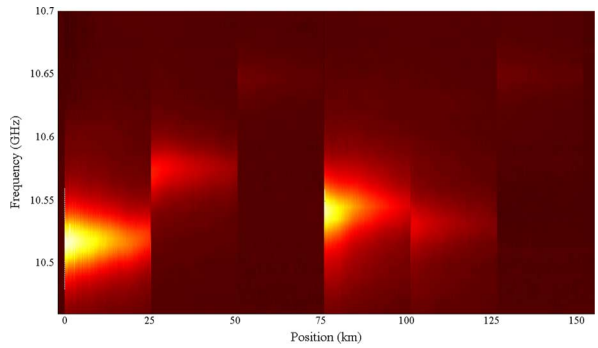


Fig. 8. Top view of the measured three-dimensional Brillouin spectra over 150-km sensing fibers.

### B. Measurement Results

The total loss (including splicing loss) of each span is measured to be ~16 dB, so the gains of EDFA1 and EDFA2 are set at ~16 dB to compensate the loss. The powers of the probe and pump waves used in experiment are set at 0.2 and 400 mW, respectively, and their frequency offset is scanned from 10460 to 10700 MHz with a step of 5 MHz. With an 80-ns pump pulse, the measured three-dimensional Brillouin spectra over the entire 150-km sensing fibers are shown in Fig. 8. The signals of the first 75 km are from the span 1 and the rest signals are from the span 2. It is clearly seen that similar Brillouin gains are shown in both two spans.

The measured Brillouin spectra at positions of 25, 50 and 75 km in each of the two spans are plotted in Fig. 9. The fitting errors of the BFS and the measured Brillouin line-widths for the two spans are listed in Table II. It is noted that compared with the results of the span 1, the Brillouin spectra obtained in the span 2 exhibit broadened line-widths and decreased signals, resulting in worse SNRs and larger fitting errors of the BFS, which is caused by the pulse spectrum broadening induced by the self-phase modulation [19], [20]. Because of the negative dispersion of MetroCor fiber, MI effect is suppressed and self-phase modulation is small in spools 1 and 2, which can be verified by the similar Brillouin line-widths of 38 and 37.8 MHz

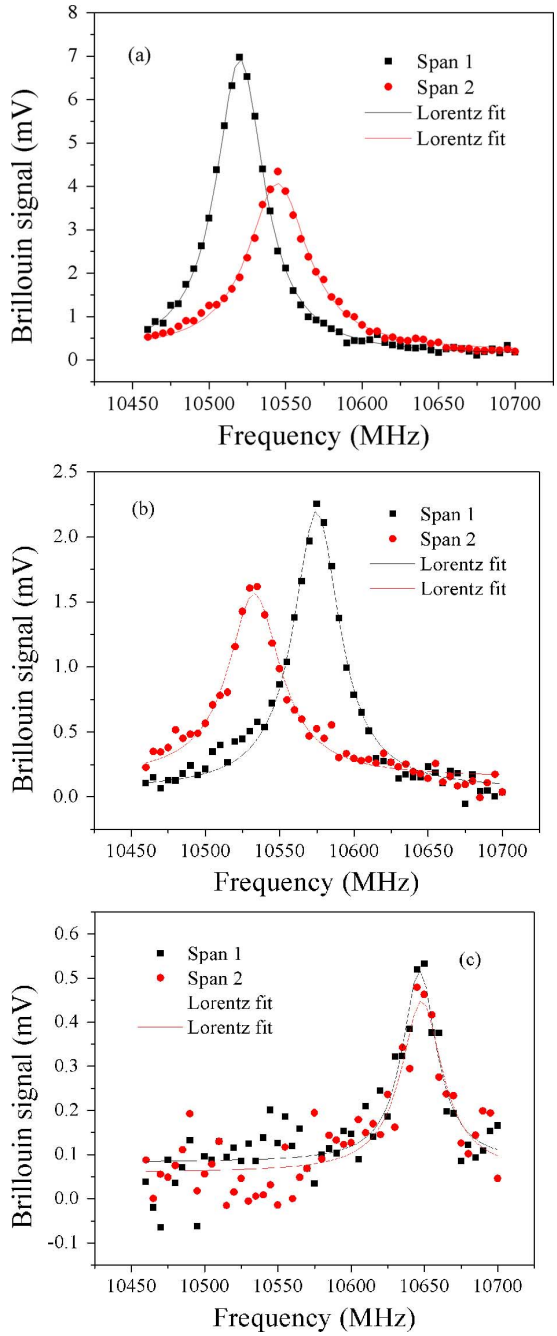


Fig. 9. Measured Brillouin spectra in two spans at the positions of (a) 25 km, (b) 50 km, and (c) 75 km.

obtained at the positions of 25 and 50 km in the span 1, respectively. However, the self-phase modulation can accumulate in both fibers, which limits the applicable pump pulse power in this scheme. As listed in Table II, the Brillouin line-widths at the ends of the two spans are measured to be 28.4 and 34.2 MHz, respectively, showing a ~6 MHz increment; while the fitting error is also increased from 1.24 to 1.49 MHz.

A 100/120 ns pulse pair is used to further improve the spatial resolution to 2 m. To verify the performance of the system, a 3-m segment near the end of the span 1 was put into an oven heated to 60°C. The measured three-dimensional Brillouin spectra in the vicinity of the heated fiber is shown in Fig. 10(a), and the Brillouin spectra of the fibers at room temperature and 60°C

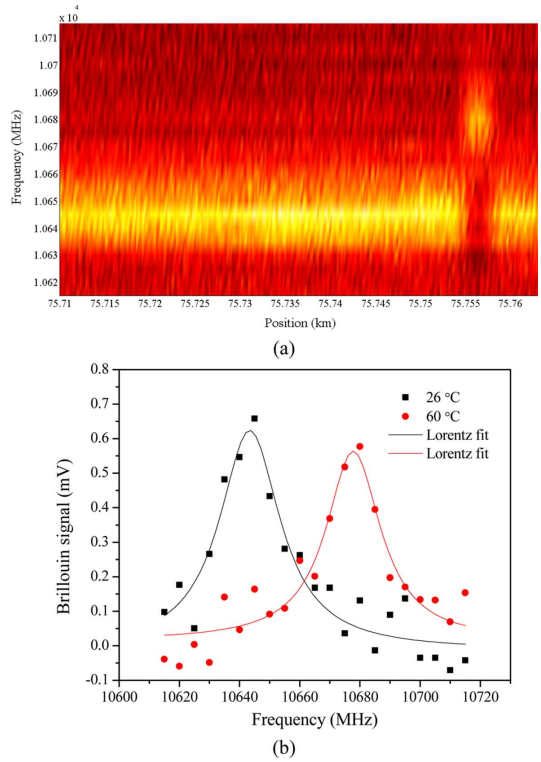


Fig. 10. (a) Three-dimensional Brillouin spectra and (b) Brillouin spectra of the fibers at room temperature and 60° C near the end of the span 1.

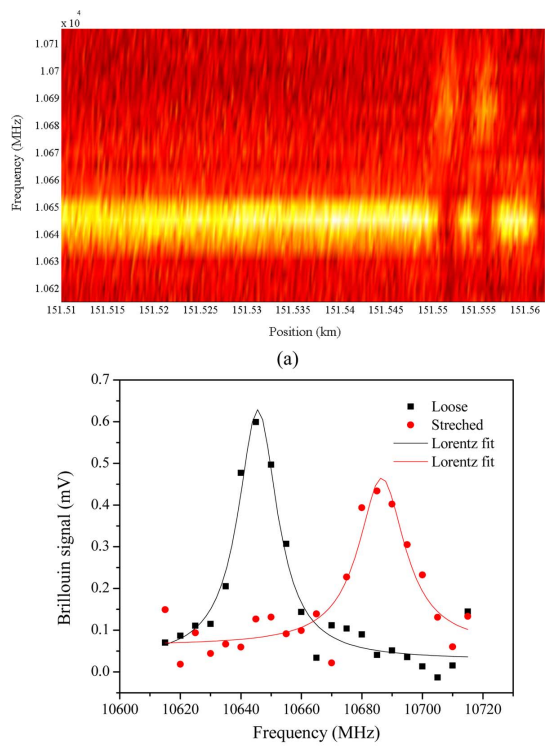


Fig. 11. (a) Three-dimensional Brillouin spectra and (b) Brillouin spectra for the fibers under loose and stretched conditions near the end of the span 2.

are plotted in Fig. 10(b), where the fitted BFSs are 10643 and 10677 MHz, respectively. In addition, two 2-m segments near the end of the span 2 were stretched simultaneously with a 2-m segment in between under loose condition, with the measured three-dimensional Brillouin spectra shown in Fig. 11(a). It is

noted that the two stretched segments and the loose one can be clearly distinguished, indicating an effective 2-m spatial resolution. The Brillouin spectra of the fibers under loose and stretched conditions are plotted in Fig. 11(b), and the corresponding BFSs are 10646 and 10687 MHz, respectively. The standard deviation of the measured BFSs near the end of the 150-km sensing fiber is calculated to be $\sim$1.5 MHz, corresponding to an accuracy of 1.5°C or 30 $\mu\varepsilon$.

## V. Conclusion

To summarize, we have demonstrated a high-performance long-range BOTDA system by combining the frequency-division multiplexing and in-line EDFAs. The frequency-division multiplexing makes use of multiple types of fibers with different BFSs to restrict the Brillouin interaction length and consequently considerably reduce the pump depletion, so that a moderate-power CW wave of BOTDA and in-line EDFAs can be used to extend the sensing range. The trade-off is a larger scanning frequency range and longer measurement time because of different scanning frequency ranges for different sections required by the frequency-division multiplexing. A 150-km sensing range has been realized by dividing the sensing fibers into two spans with one optical repeater including two in-lines EDFAs, and more spans would be expected to further extend the sensing range, which is under investigation.

## References


[1] T. Horiguchi, K. Shimizu, T. Kurashima, M. Tateda, and Y. Koyamada, "Development of a distributed sensing technique using Brillouin scattering," *J. Lightw. Technol.*, vol. 13, no. 7, pp. 1296–1302, Jul. 1995.

[2] M. N. Alahbabi, Y. T. Cho, T. P. Newson, P. C. Wait, and A. H. Hartog, "Influence of modulation instability on distributed optical fiber sensors based on spontaneous Brillouin scattering," *J. Opt. Soc. Amer. B*, vol. 21, pp. 1156–1160, 2004.

[3] E. Geinitz, S. Jetschke, U. Ropke, S. Schroter, R. Willsch, and H. Bartelt, "The influence of pulse amplification on distributed fiber-optic Brillouin sensing and a method to compensate for systematic errors," *Meas. Sci. Technol.*, vol. 10, pp. 112–116, 1999.

[4] Y. Dong, L. Chen, and X. Bao, "System optimization of a long-range Brillouin loss-based distributed fiber sensor," *Appl. Opt.*, vol. 49, pp. 5020–5025, 2010.

[5] M. A. Soto, G. Bolognini, F. D. Pasquale, and L. Thevenaz, "Simplex-coded BOTDA fiber sensor with 1 m spatial resolution over a 50 km range," *Opt. Lett.*, vol. 35, pp. 259–261, 2010.

[6] H. Liang, W. Li, N. Linze, L. Chen, and X. Bao, "High-resolution DPP-BOTDA over 50 km LEAF using return-to-zero coded pulses," *Opt. Lett.*, vol. 35, pp. 1503–1505, 2010.

[7] M. A. Soto, G. Bolognini, and F. D. Pasquale, "Long-range simplex-coded BOTDA sensor over 120 km distance employing optical preamplification," *Opt. Lett.*, vol. 36, pp. 232–234, 2011.

[8] X. H. Jia, Y. J. Rao, L. Chen, C. Zhang, and Z. L. Ran, "Enhanced sensing performance in long distance Brillouin optical time-domain analyzer based on Raman amplification: Theoretical and experimental investigation," *J. Lightw. Technol.*, vol. 28, no. 11, pp. 1624–1630, Jun. 2010.

[9] F. R. Barrios, S. M. Lopez, A. C. Sanz, P. Corredera, J. D. A. Castanon, L. Thevenaz, and M. G. Herraez, "Distributed Brillouin fiber sensor assisted by first-order Raman amplification," *J. Lightw. Technol.*, vol. 28, no. 15, pp. 2162–2172, Aug. 2010.

[10] M. A. Soto, G. Bolognini, and F. D. Pasquale, "Optimization of long range BOTDA sensors with high resolution using first-order bidirectional Raman amplification," *Opt. Express*, vol. 19, pp. 4444–4457, 2011.

[11] Y. Dong, L. Chen, and X. Bao, "Time-division multiplexing-based BOTDA over 100 km sensing length," *Opt. Lett.*, vol. 36, pp. 277–279, 2011.

[12] A. Minardo, R. Bernini, and L. Zeni, "A simple technique for reducing pump depletion in long-range distributed Brillouin fiber sensors," *IEEE Sens. J.*, vol. 9, no. 6, pp. 633–634, Jun. 2009.

[13] L. Thevenaz, S. F. Mafang, and J. Lin, "Depletion in a distributed Brillouin fiber sensor: Practical limitation and strategy to avoid it," in *Proc. 21st Int. Conf. Opt. l Fiber Sensors*, Ottawa, ON, Canada, 2011, POst-deadline Paper 5, SPIE.

[14] Y. Dong, X. Bao, and L. Chen, "High-performance Brillouin strain and temperature sensor based on frequency-division multiplexing using nonuniform fibers over 75-km fiber," in *Proc. 21st Int. Conf. Opt. Fiber Sens.*, Ottawa, ON, Canada, 2011, p. 77533H, SPIE.

[15] A. B. Ruffin, M. J. Li, X. Chen, A. Kobyakov, and F. Annunziata, "Brillouin gain analysis for fibers with different refractive indices," *Opt. Lett.*, vol. 30, pp. 3123–3125, 2005.

[16] L. Thevenaz and S. F. Mafang, "Distributed fiber sensing using Brillouin echoes," in *Proc. 19th Int. Conf. Opt. Fiber Sens.*, Perth, WA, Australia, 2008, p. 70043N, SPIE.

[17] W. Li, X. Bao, Y. Li, and L. Chen, "Differential pulse-width pair BOTDA for high spatial resolution sensing," *Opt. Exp.*, vol. 16, pp. 21616–21625, 2008.

[18] Y. Dong, X. Bao, and W. Li, "Differential Brillouin gain for improving the temperature accuracy and spatial resolution in a long-distance distributed fiber sensor," *Appl. Opt.*, vol. 48, pp. 4297–4301, 2009.

[19] V. Lecoeuche, D. J. Webb, C. N. Pannell, and D. A. Jackson, "25 km Brillouin based single-ended distributed fiber sensor for threshold detection of temperature or strain," *Opt. Commun.*, vol. 168, pp. 95–102, 1999.

[20] S. M. Foaleng, F. Rodriguez-Barrios, S. Martin-Lopez, M. Gonzalez-Herraez, and L. Thevenaz, "Detrimental effect of self-phase modulation on the performance of Brillouin distributed fiber sensors," *Opt. Lett.*, vol. 36, pp. 97–99, 2011.



**Yongkang Dong** received the Ph.D. degree in physical electronics from Harbin Institute of Technology, Harbin, China, in 2008.

Since 2008, he has been working as a Post-doctoral Fellow in the Physics Department, University of Ottawa, ON, Canada. His current research interests involve nonlinear fiber optics and Brillouin scattering in optical fibers and its applications for sensing.

**Xiaoyi Bao** (SM'04) received the B.Sc. and M.Sc. degrees in physics from Nankai University, China, in 1982 and 1985, respectively, and the Ph.D. degree in optics from Anhui Institute of Optics and Fine Mechanics, Academic Sinica, in 1987.

She joined the Physics Department, University of Ottawa, Ottawa, ON, Canada, in 2000 as a Full Professor and became Tier I Canada Research Chair in Fiber Optics and Photonics in 2002. Her research involves nonlinear effects in optical fibers and their applications for sensing, device and communications. She has authored and coauthored more than 320 journal papers and international conference presentations.

Prof. Bao is a Fellow of the Royal Society of Canada (RSC) and secretary of Academy of Science (2009–2011). She was Applied Physics Division Chair of Canadian Association of Physics in 1998, and served on NSERC (Natural Science Research Council of Canada) Council from 1998–2001. She was the recipient of the Ontario Premier's Research Excellence Award in 2001, the Ontario Distinguished Researcher Award in 2002, the 1st University of Ottawa Inventor of the Year Award in 2003, Researcher of the Year 2004 from Faculty of Science (U of Ottawa), the National Centers of Excellence Chair's Medal in 2006, and the Canadian Association of Physics (CAP)-National Optics Institute (NOI) Medal for Outstanding Achievement in Applied Photonics in 2010.